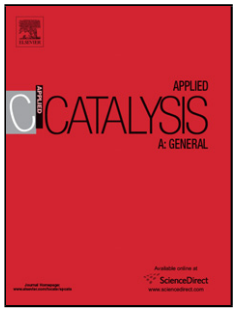

Title: Influence of the support of copper catalysts on activity and 1,2-dichloroethane selectivity in ethylene oxychlorination

Authors: Zuzana Vajglová, Narendra Kumar, Kari Eränen, Anton Tokarev, Markus Peurla, Janne Peltonen, Dmitry Yu. Murzin, Tapio Salmi

PII: S0926-860X(18)30070-X
DOI: https://doi.org/10.1016/j.apcata.2018.02.012
Reference: APCATA 16552

To appear in: *Applied Catalysis A: General*

Received date: 23-11-2017
Revised date: 7-2-2018
Accepted date: 12-2-2018

Please cite this article as: Vajglová Z, Kumar N, Eränen K, Tokarev A, Peurla M, Peltonen J, Murzin DY, Salmi T, Influence of the support of copper catalysts on activity and 1,2-dichloroethane selectivity in ethylene oxychlorination, *Applied Catalysis A, General* (2010), https://doi.org/10.1016/j.apcata.2018.02.012

Influence of the support of copper catalysts on activity and 1,2-dichloroethane selectivity in ethylene oxychlorination

Zuzana Vajglová[a,b], Narendra Kumar[a], Kari Eränen[a], Anton Tokarev[a], Markus Peurla[c], Janne Peltonen[c], Dmitry Yu. Murzin[a,*], Tapio Salmi[a]

[a] *Åbo Akademi University, Johan Gadolin Process Chemistry Centre, Laboratory of Industrial Chemistry and Reaction Engineering, Biskopsgatan 8, Turku/Åbo, Finland*

[b] *Institute of Chemical Process Fundamentals of the ASCR, v. v. i., Eduard Hála Laboratory of Separation Processes, Rozvojova 2/135 Prague 6, Czech Republic*

[c] *University of Turku, Turku, Finland*

[*] *Corresponding author: dmurzin@abo.fi*

Graphical abstract

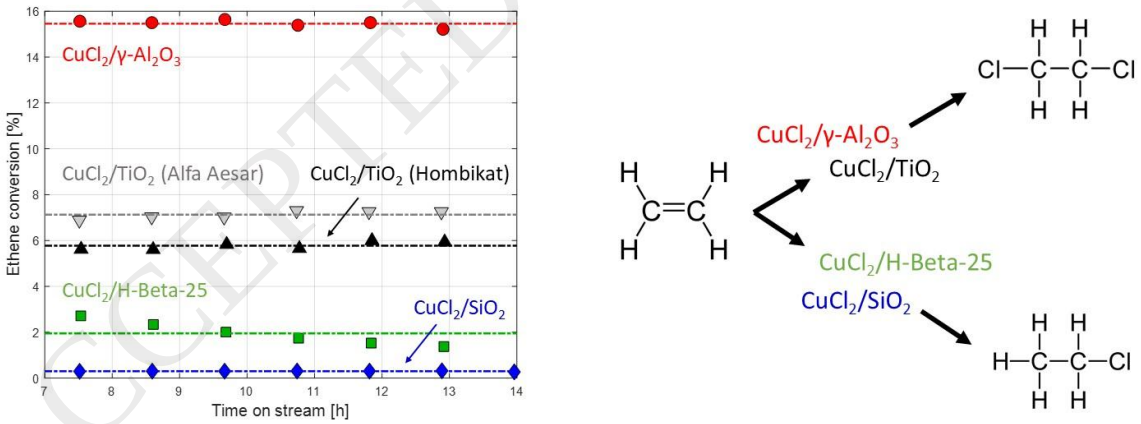

Highlights

- Five $CuCl_2$ catalysts were compared in ethylene oxychlorination.
- Extensive physical-chemical analysis was done
- Catalysts with γ-Al_2O_3 and TiO_2 as supports demonstrated very good activity and 1,2-dichloroethane selectivity.
- Zeolite H-Beta-25 and SiO_2 as support materials were unusable for ethylene oxychlorination.

Abstract

Five different support materials were modified with 5 wt.% Cu, using an evaporation impregnation method. The synthesized $CuCl_2/\gamma$-Al_2O_3, $CuCl_2/TiO_2$ (Hombikat), $CuCl_2/TiO_2$ (Alfa Aesar), $CuCl_2/SiO_2$ and $CuCl_2$/H-Beta-25 materials were characterized by nitrogen physisorption, X-ray powder diffraction, scanning electron microscopy, energy dispersive X-ray microanalysis, transmission electron microscopy, Fourier transform infrared spectroscopy and CO_2-temperature programmed desorption. The physical-chemical characterization was correlated with catalytic activity, stability and selectivity in the ethylene oxychlorination. It was found that γ-Al_2O_3 and TiO_2 support materials demonstrate very good activity and 1,2-dichloroethane selectivity compare to other catalysts. Zeolite H-Beta-25 and SiO_2 support materials proved to be unusable for this reaction.

Keywords: oxychlorination, copper, support effect, alumina, titania, zeolite

1 Introduction

The heterogeneously catalyzed gas-phase ethylene oxychlorination by oxygen and hydrogen chloride to 1,2-dichloroethane (1,2-DCEA) over supported copper(II) chloride catalysts is one of the principal steps in the industrial production of an important monomer chloroethene (vinyl

chloride, VC), needed for synthesis of poly-vinyl chloride (PVC). This a versatile plastic material is produced with worldwide production of 44 M ton per year [1-7].

A highly exothermic oxychlorination ($\Delta H^0_{R,298K} = -295$ kJ/mol) and formation of volatile copper chloride are two factors which have to be taken into account during process development [4]. Therefore, temperature control is essential to limit the sublimation rate of copper chlorides, prevent rapid catalyst deactivation and to ensure high selectivity to 1,2-dichloroethane. Indeed, onset of selectivity loss due to further oxychlorination and oxidation reactions is found above 240 °C. The main by-products being ethyl chloride, 1,1,2-trichloroethane, trichloroacetaldehyde, tetrachlormethane, trichloromethane, carbon monoxide, and carbon dioxide. Vinyl chloride, chloromethane, dichloromethane, 2-chloroethanol, 1,2-dichloroethylenes (cis/trans), 1,1-dichloroethane, and 1,1,2,2-tetrachloroethane are also formed, but only in minor amounts. Trichloroacetaldehyde is the least desirable product, due to the difficulty of its separation and a need to create a special unit for its decomposition with an alkali solution [8]. The detailed chlorination mechanism generating such a wide variety of by-products and determining the process selectivity is likely a result of a combination of parallel and successive oxychlorination and hydrochlorination steps. An open debate still exists about the origin of carbon oxides: under oxidative conditions in the absence of HCl. Ethylene oxychlorination is commonly performed at temperature 200 – 300 °C at 1 – 10 bar in fluidized-bed reactors [4, 7, 8].

Despite many decades of research and commercial experience, the catalysts for ethylene oxychlorination are still under investigation. Promoted $CuCl_2$-containing catalysts are commonly used in oxychlorination. Commercial oxychlorination catalysts are synthesized by impregnation of γ-Al_2O_3 with $CuCl_2$ (4 − 16 wt % Cu). Besides the active phase a range of promoters, for example, K, Na, and La are applied [4]. There is now a general agreement that the overall mechanism involves a copper oxychloride intermediate in the redox process where

copper is cycled between Cu(I) and Cu(II) oxidation states, being periodically reduced by ethylene and reoxidized by oxygen [1-7]:

$$C_2H_4 + 2CuCl_2 \longrightarrow C_2H_4Cl_2 + 2CuCl \quad (1)$$

$$2CuCl + \tfrac{1}{2}O_2 \longrightarrow CuO{\cdot}CuCl_2 \quad (2)$$

$$CuO{\cdot}CuCl_2 + 2HCl \longrightarrow 2CuCl_2 + H_2O \quad (3)$$

The active site probably comprises an isolated Cu_xCl_y complex, which is anchored to a high-surface-area catalyst support. One of the main challenges of this process is Cu^{1+} deposits on the catalyst surface during the reaction, causing aggregation and loss of Cu due to its low melting temperature and volatility. Therefore, alkali metal compounds such as K, Na, and/or rare earth metals e.g. La are often used as promoters to increase the activity, selectivity, and stability of $CuCl_2$-based catalysts in industrial reactors [4, 9, 10]. Despite the use of rare earth and alkali metal chlorides as promoters and the mature state of the process there is still a substantial product loss (up to 10%) because of side and secondary reactions leading to CO, CO_2 and C_1 and C_2 chlorohydrocarbons [1, 2, 10-12].

Selectivity is the main governing factor, determining the technological and, finally, economic efficiency of the process. In the best operating regimes, chlorine selectivity exceeds 99%; ethylene selectivity is 96 – 98%, depending on the oxidizer, which is either oxygen or air. The significance of high selectivity is illustrated, for example, by the fact that an increase of ethylene selectivity by 1% in the vinyl chloride production with a capacity of 300000 t/yr results in ethylene savings of ca. 800 t/yr [13].

Therefore, the present study is devoted to elucidation of catalytic performance, especially selectivity of 1,2-dichloroethane, in relation to the catalyst support type which is not addressed in the literature so far. Moreover, tested catalysts were devoid of any promoters making

elucidation of the role of the support in activity, stability and selectivity more apparent. This work and an on-going study of oxychlorination in a microchannel reactor represents further effort to elucidate the parameters influencing catalytic behaviour.

2 Experimental

2.1 Catalyst synthesis

Five different supports were used, namely γ-alumina (γ-Al_2O_3 VGL-25, UOP Inc.), silica gel (SiO_2, Merck & Co., Inc.), titanium dioxide Hombikat (TiO_2 Hombikat UV-100, anatase and rutile, Sigma Aldrich), titanium dioxide Alfa Aesar (TiO_2, anatase, Alfa Aesar GmbH) and NH_4-Beta-25 zeolite (CP814E, 25 = SiO_2/Al_2O_3 molar ratio, Zeolyst International). The NH_4^+ form of zeolite was transformed to the corresponding proton form in a muffle oven by using a step calcination procedure: initial temperature 250 °C held for 50 min and then increased at 4 °C/min to 400 °C and held at the final temperature for 4 h. Before synthesis of catalysts, the support materials were crushed and sieved into a fraction < 63 μm in a vibratory micro mill (Fritsch).

The synthesis procedure was the same for all catalysts. As a method of cupric chloride introduction a conventional evaporation impregnation method (EIM) was used. In all cases copper(II) chloride dihydrate ($CuCl_2 \cdot 2H_2O$, p.a., Honeywell) was used as a precursor. The catalyst synthesis was carried out using a constant concentration in a stirred bath containing 250 mL of 0.02 M aqueous solution and 5 g of the catalyst support. The solution was rotated for 24 h at 60 °C, and subsequently, water was evaporated at 40 °C under vacuum. The copper-modified catalysts with a nominal loading of 5 wt. % was dried in an oven at 100 °C for 7 h, and calcined in a step calcination procedure: initial temperature 250 °C held for 50 min and then increased at 4 °C/min to 450 °C and held at the final temperature for 3 h.

2.2 Catalyst characterization

2.2.1 Nitrogen physisorption

The specific surface area of supports and copper chloride containing catalysts was determined by nitrogen-physisorption using Sorptometer 1900 (Carlo Erba Instruments). The sample was outgassed at 150 °C for 3 h before each measurement. The BET and Dubinin equations were used for calculation of the specific surface area of the mesoporous materials and microporous zeolites, respectively. The pore volumes were calculated with the Dollimore-Heal method [14] for mesoporous material and the Horvath-Kawazoe method [15] for microporous zeolites.

2.2.2 Fourier transform infrared spectroscopy (FTIR)

The amount of Lewis and Brønsted acid sites on the copper chloride modified catalysts was quantified by Fourier transform infrared spectroscopy using pyridine (≥ 99.5%) as the probe molecule (ATI Mattson FTIR Infinity Series). The samples were pressed into thin pellets (10 – 20 mg) and placed in the measurement cell. Prior to the pyridine adsorption, the samples were outgassed under vacuum (0.08 mbar) at 450 °C for 2 h and the background spectra were recorded at 100 °C. The strength of acid sites was classified depending on pyridine desorption temperature, i.e. desorption at 250 and 350 °C was assigned to weak and medium acid sites respectively. Strong acid sites retain pyridine at 450 °C. The Lewis acidity was determined from the adsorption band at 1450 cm^{-1} and the Brønsted acidity from the adsorption band at 1550 cm^{-1} using the molar extinction parameters previously reported by Emeis [16].

2.2.3 Scanning electron microscopy (SEM) and energy dispersive X-ray microanalysis (EDX)

Morphological studies were performed by scanning electron microscopy. A scanning electron microscope (Zeiss Leo Gemini 1530) was used for determination of the crystal morphology of the proton forms and copper chloride containing catalysts.

The copper and chlorine content was investigated by energy-dispersive X-ray microanalysis (Zeiss Leo Gemini 1530).

2.2.4 Transmission electron microscopy (TEM)

The catalysts were characterized by transmission electron microscopy (JEOL JEM-1400Plus) using imaging and electron diffraction functions. The samples were prepared by blowing a powder on the TEM grid with a pipette.

2.2.5 Temperature programme desorption (TPD) of CO_2 and NH_3

The basicity of the catalysts was studied by performing temperature programme desorption of CO_2 (CO_2-TPD, Micromeritics Instrument AutoChem 290) using a conventional flow-through reactor with CO_2 as a probe molecule. The catalyst was first dried under helium flow, followed by adsorption of CO_2, flushing away physisorbed CO_2 and temperature programmed desorption up to 900 °C. The eluent from the reactor was analysed by a thermal conductivity detector.

The acidity of TiO_2 pristine supports and Cu modified TiO_2 catalysts were studied by TPD using NH_3 as a probe molecule with a procedure similar to that of CO_2-TPD.

2.2.6 X-ray powder diffraction

The catalyst crystal structure was determined by X-ray diffraction (XRD) with a Philips X'Pert Pro MPD X-ray powder diffractometer. The device was operated in Bragg-Brentano diffraction mode, and the monochromatized Cu-Kα radiation (λ = 1.541874 Å) was generated with a voltage of 40 kV and a current of 45 mA. The measured 2θ angle range was 5.0°−85.0°, with a step size of 0.026° and measurement time of 100 s per step. The measured diffractograms were analyzed with Philips X'Pert HighScore and MAUD programs. HighScore together with MAUD was used for the phase analysis and MAUD for the Rietveld refinement.

2.3 Catalytic tests of the ethylene oxychlorination

2.3.1 Experimental setup

The reaction was carried out in a quartz tubular reactor with a length of 30 cm and an inner diameter of 1 cm. A catalyst sample of 0.5 g with the size 250 – 500 µm was mixed with 8.5 g of inert glass beads. This mixture was loaded into the reactor as a fixed bed between glass beads and quartz wool. The length of the catalyst bed was 10 cm. In order to determine whether the internal diffusion is limiting the reaction, the Weisz–Prater criterion (WP) was used [17]. The calculated Weisz-Prater criterion was 0.0004 for the measurement over $CuCl_2/\gamma\text{-}Al_2O_3$ with the size 250 – 500 µm at 250 °C, which means that diffusion limitations in the pores of the catalyst particles can be excluded.

The reaction system is illustrated in Figure 1. The reactor was equipped with a thermocouple positioned close to the catalytic bed to record the gas-phase temperature. Swagelok stainless steel lines and valves were used in the equipment. All the lines after reactor were isolated and heated to 120 °C.

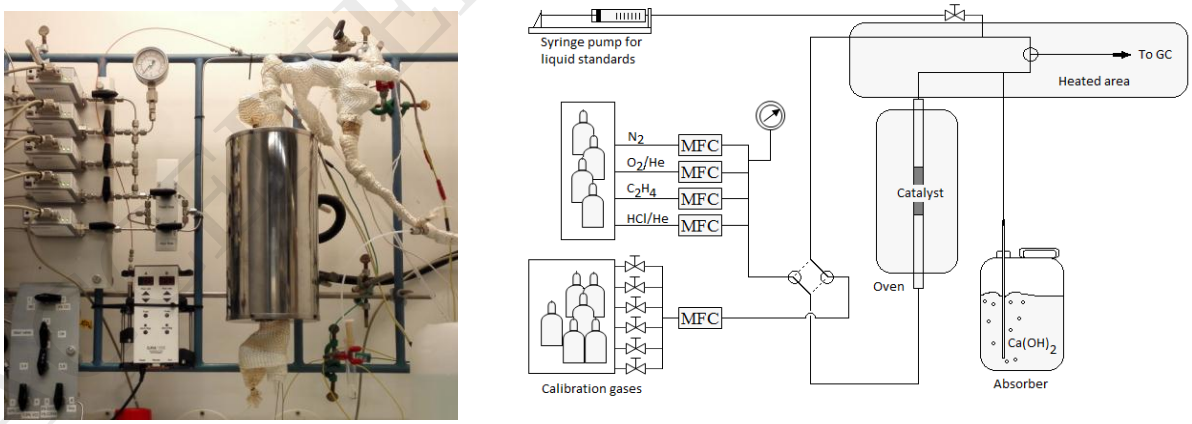

Figure 1. Schematic presentation of the fixed bed reactor for catalyst evaluation.

The reaction was conducted at 200 – 250 °C and under atmospheric pressure, with a weight space velocity (WHSV) of 0.9 $g(C_2H_4)/g(cat)/h$ and residence time 5 s. The reaction

temperature program for catalyst screening consisted of two parts. During the first phase, the catalyst was pre-treated in a nitrogen flow rate of 10 NmL/min (STP) by heating it with the rate of 4 °C/min up to 250 °C for 2 h. In the second phase, ethylene oxychlorination proceeded subsequently at different temperatures (200 °C, 225 °C, 250 °C and 200 °C) for at least 7 h at each temperature. The total flow rate was 20 NmL/min being composed from: 6.1 NmL/min C_2H_4 (AGA Industrial Gases), 2.7 NmL/min O_2/He (AGA Industrial Gases, 19.8%), 10 NmL/min HCl/He (AGA Industrial Gases, 19%), 1.2 NmL/min N_2 (AGA Industrial Gases). A nitrogen with the content of 6% was used as an inert standard for GC analysis, while helium (51.4%) was used as a balance gas. At the reactor outlet, a large amount of the reaction mixture was fed to the calcium hydroxide absorber. Both measures, diluting the reaction mixture with inert gases (He + N_2) and analysing only a small portion of the reaction stream were used to avoid corrosion of the device. The apparatus was heated to prevent partial condensation of any gas component. Mass flow controllers (Bronkhorst EL-flow) controlled the gas flow.

2.3.2 Analytical method

The gaseous products were analyzed on-line applying Agilent GC 6890N equipped with FID and TCD detectors and HP-Plot/U Column (30 m × 530 µm × 20 µm), molsieve/Column (60 m × 50 µm × 20 µm). Injection was performed a six-way valve. The transfer line temperature was held at 150 °C and the temperature program started at 50 °C for 10 min followed by a temperature gradient to 185 °C at a ramp 6 °C/min, holding 18.6 min and then increasing to 190 °C at a ramp 10 °C/min with subsequent holding for 7 min. The mobile phase was helium. Temperatures of FID and TCD detectors were 300 °C and 250 °C, respectively. Continuous GC analysis was applied with a sampling frequency of 65 min.

3 Results and discussion

3.1 Catalyst characterization results

3.1.1 Effect of copper loading on the surface area and pore volume

The specific surface areas and pore volumes of the catalysts were determined by nitrogen physisorption, before and after impregnation with $CuCl_2$, as well as spent and regenerated Cu modified catalysts. The results are summarized in Table 1.

Upon modification with copper, the surface area and the pore volume were as expected decreased due to pore blocking. Blocking of some micro- or mesopores can be attributed to the bulk copper species (large particles of CuO) or eventually also to the support hydrolysis during impregnation. Lower specific surface areas were measured for $CuCl_2/TiO_2$ (Alfa Aesar) (by 82%), $CuCl_2/TiO_2$ (Hombikat) (by 30%) and $CuCl_2$/H-Beta-25 (by 25%) catalysts. For $CuCl_2/\gamma$-Al_2O_3, the decrease of the surface area was ca. 10%, as compared to the pristine support. The mesoporous $CuCl_2/TiO_2$ (Alfa Aesar) catalyst exhibited the lowest specific surface areas while the microporous $CuCl_2$/H-Beta-25 catalyst displayed the highest one.

Table 1. Specific surface area and pore volume of catalysts before and after impregnation with $CuCl_2$, and of spent and regenerated Cu modified catalysts.

Catalyst	**Porosity**	**Specific surface area, m^2/g**				**Specific pore volume, cm^3/g**			
		Neat	*Fresh*	*Spent*	*Reg.*	*Neat*	*Fresh*	*Spent*	*Reg.*
			$CuCl_2$/support				*$CuCl_2$/support*		
$CuCl_2/\gamma$-Al_2O_3	meso	286	260	105	120	1.15	0.89	0.21	0.27
$CuCl_2/TiO_2$ (Hombikat)	meso	44	31	12	9	0.23	0.13	0.06	0.05
$CuCl_2/TiO_2$ (Alfa Aesar)	meso	150	26	6	52	0.37	0.12	0.02	0.07
$CuCl_2/SiO_2$	meso	336	275	102	112	0.69	0.51	0.12	0.20
$CuCl_2$/H-Beta-25	micro	1102	827	133	348	0.85	0.69	0.24	0.33

The specific surface areas of the spent $CuCl_2$ catalysts were significantly lower than those for the fresh $CuCl_2$ catalysts, which may be attributed to partial blocking of the pores by coke formation during the reaction. Compared with the fresh catalysts, these decreases were higher than 60%, reaching for the Beta catalyst even more than 80%.

Regeneration of $CuCl_2/\gamma$-Al_2O_3, $CuCl_2/SiO_2$ and $CuCl_2$/H-Beta-25 catalysts resulted in partial restoration of the specific surface area. In the case of $CuCl_2/TiO_2$ (Alfa Aesar), the specific surface after regeneration was even higher than the initial value.

3.1.2 Effect of copper loading on acidity

Acidity of the catalysts, before and after impregnation with $CuCl_2$, was measured by FTIR spectroscopy using pyridine as the probe molecule. The acidity data are given in Table 2. For Cu modified TiO_2 catalysts and pristine TiO_2 support materials, FTIR could not be used because the catalytic pellets prepared for analysis were too fragile. For this reason, the acidity of these samples was characterized with temperature programme desorption using ammonia as a probe molecule, therefore in Table 2, only the total acidity data are given.

Table 2. Determination of acidic properties of acid sites using FTIR-pyridine.

	Brønsted acidity, µmol/g				**Lewis acidity, µmol/g**				**Total acidity**
Catalyst	*weak* *250 °C*	*medium* *350 °C*	*strong* *450 °C*	∑	*weak* *250 °C*	*medium* *350 °C*	*strong* *450 °C*	∑	*µmol/g* *250 – 450 °C*
γ-Al_2O_3	1	1	1	2	17	17	6	41	43
$CuCl_2/\gamma$-Al_2O_3	70	2	0.3	**72**	173	54	1	**229**	**301**
TiO_2 (Hombikat)	n.a.	n.a.	n.a.	n.a.	n.a.	n.a.	n.a.	n.a.	89*
$CuCl_2/TiO_2$ (Hombikat)	n.a.	n.a.	n.a.	n.a.	n.a.	n.a.	n.a.	n.a.	**92***
TiO_2 (Alfa Aesar)	n.a.	n.a.	n.a.	n.a.	n.a.	n.a.	n.a.	n.a.	144*

$CuCl_2/TiO_2$ (Alfa Aesar)	n.a.	n.a.	n.a.	n.a.	n.a.	n.a.	n.a.	n.a.	**107***
SiO_2	0.5	0.5	0.4	1	0.2	0.2	0.1	1	2
$CuCl_2/SiO_2$	1	1	3	**4**	22	1	1	**23**	**27**
H-Beta-25	118	124	101	342	37	40	34	112	454
$CuCl_2$/H-Beta-25	157	18	0.3	**175**	246	39	0.2	**285**	**460**

* Evaluated using temperature-programmed desorption of ammonia (NH_3-TPD)

Upon modification with copper, catalysts exhibited substantial increases in the amount of the weak Brønsted acid sites and total Lewis acidity (Table 2). Compared to the pristine support, total Lewis acidity was increased 23 times, 5.6 times and 2.5 times for $CuCl_2/SiO_2$, $CuCl_2/\gamma$-Al_2O_3 and $CuCl_2$/H-Beta-25, respectively. The increase in the Lewis acid sites is attributed to the presence of Cu species in the catalysts. This is consistent with the work of Finocchio et al. [2]. A plausible explanation for the enhancement in the weak Brønsted acid can be presence of Cl^- in the Cu-modified catalysts even of the calcination at 400 °C in the muffle oven (Table 4).

On the contrary, the amount of the strong acid sites after introduction of Cu was significantly decreased, except for the strong Lewis acid sites in $CuCl_2/SiO_2$ catalyst. Current investigations of the metal-modified catalysts show that a decrease reduction of the acid site strength is not limited only to Cu and the supports reported here, similar trends have been observed also by others for Pt, Ir, Ru and Rh supported on various acidic supports [18].

The highest increase in the total Brønsted and Lewis acid concentration was determined for $CuCl_2/\gamma$-Al_2O_3 (seven times higher as compared to the pristine support). The total acidity for $CuCl_2$/H-Beta-25 compared to the pristine support remained almost unchanged. For all Cu modified catalysts measured by the FTIR method, the Lewis acidity was higher than the Brønsted acidity.

3.1.3 Effect of copper loading on the formation of basic sites

The amount of basic sites on the surface of $CuCl_2$ containing catalysts was determined by temperature programme desorption (TPD) of carbon dioxide as a probe molecule (Table 3). The amount of weak, medium and strong basic site was estimated from the peak areas under TPD curves for the temperature range of 370 – 500 K, 500 – 750 K, and 750 – 1170 °C, respectively.

Table 3. The relative amounts of CO_2 from the supported Cu catalysts determined by CO_2.

Catalyst	**Basic site, mmol/g**			**Total basicity**
	weak	*medium*	*strong*	*mmol/g*
	370 - 500 K	*500 - 750 K*	*750 - 1170 K*	*370 - 1170 K*
γ-Al_2O_3 [19]	3.0	1.7	4.9	9.6
$CuCl_2/\gamma$-Al_2O_3	0.4	1.2	8.9	**10.5**
TiO_2 (Alfa Aesar) [19]	0.1	0.5	0.1	0.7
$CuCl_2/TiO_2$ (Hombikat)	0.1	0.9	2.5	**3.6**
$CuCl_2/TiO_2$ (Alfa Aesar)	0.1	0.6	3.7	**4.3**
SiO_2 [19]	0.2	0.1	0.4	0.7
$CuCl_2/SiO_2$	0.1	0.4	8.8	**9.3**
$CuCl_2$/H-Beta-25	0.1	0.2	5.5	**5.8**

For all types of catalysts, upon modification with copper, the amount of basic site was increased. This trend has been observed also for CeO_2 modified catalyst [17]. The highest amount of total basic sites was observed for $CuCl_2/\gamma$-Al_2O_3 (10.5 mmol/g) catalyst followed by $CuCl_2/SiO_2$ (9.3 mmol/g). All Cu-modified catalysts exhibited the highest percentage of the strong basic sites.

The highest increase in the amount of total basic sites upon modification with $CuCl_2$ was obtained for $CuCl_2/SiO_2$ (13.3 times higher as compared to the pristine support). The second

highest increase in the basic sites was obtained for $CuCl_2/TiO_2$ (Alfa Aesar) (6.2 times higher as compared to the pristine support). Hence, it can be concluded that the creation of basic sites was influenced by the structure of support and its intrinsic basic characteristics.

Contrary to SiO_2 and TiO_2 having small amounts of basic sites (0.7 mmol/g), γ-Al_2O_3 exhibited the highest amount of total basic sites (9.6 mmol/g). However, this support on modification with $CuCl_2$ exhibited only partial enhancement in basic sites (10.5 mmol/g) i.e. increase with only 1 mmol/g for the $CuCl_2/\gamma$-Al_2O_3.

3.1.4 Effect of copper loading on support morphology and copper particle size

$CuCl_2$ catalysts were prepared with the nominal Cu loading of 5 wt.% and respective Cl loading of 2.8 wt.% using $CuCl_2 \cdot 2H_2O$ as a precursor. The content of Cu and Cl in wt.% as well as the Cl/Cu atomic ratio determined by energy dispersive X-ray microanalysis are given in Table 4. The results are close to this nominal loading (5.12 ± 0.16 wt.% of Cu for $CuCl_2/\gamma$-Al_2O_3), indicating that the impregnation method used for the metal introduction was successful. A slightly higher measured value is probably related to precision of analysis. For other catalysts, the content of Cu was slightly lower than the nominal loading. The lowest Cu content was measured for SiO_2 (2.51 ± 0.13 wt.% of Cu).

For all catalysts, the Cl/Cu atomic ratio was significantly lower than two. This indicates that most of copper is not present as $CuCl_2$ on the surface but reacts with the support surface or forms separate particles of oxygen- containing copper species as CuO or copper chloride hydroxide. The highest Cl/Cu atomic ratio (0.44) was observed with γ-Al_2O_3 as a support. In other cases, the Cl/Cu ratio was significantly lower (< 0.2) or Cl was not detected at all.

Table 4. SEM-EDX, TEM: $CuCl_2$ catalyst, nominal Cu loading 5 wt.% and nominal Cl loading 2.8 wt.%.

Catalyst	**Cu**	**Cl**	**Cl/Cu**	**Support crystallite size, nm**	**Copper size, nm**

	wt.%	*wt.%*	*at/at*	*min - max*	*avg*	*min - max*	*avg*
$CuCl_2/\gamma\text{-}Al_2O_3$	5.12±0.16	1.28±0.03	**0.44**	44 - 184	114	3.1 - 9.2	**5.8**
$CuCl_2/TiO_2$ (Hombikat)	3.01±0.11	0.18±0.03	**0.10**	47 - 131	77	1.1 - 6.0	**2.6**
$CuCl_2/TiO_2$ (Alfa Aesar)	2.64±0.12	-	-	44 - 106	60	1.1 - 7.6	**4.7**
$CuCl_2/SiO_2$	2.51±0.13	0.21±0.02	**0.15**	43 - 251	66	3.1 - 11.3	**5.0**
$CuCl_2$/H-Beta-25	3.99±0.15	-	-	33 - 152	46	3.1 - 11.3	**4.7**

Scanning electron microscopy was used to study the morphology (shape, size and distributions) of Cu modified $\gamma\text{-}Al_2O_3$, TiO_2 (Hombikat), TiO_2 (Alfa Aesar), SiO_2 and H-Beta-25 catalysts (Figure 2). The average crystal sizes of the catalysts are given in Table 4, being rather similar.

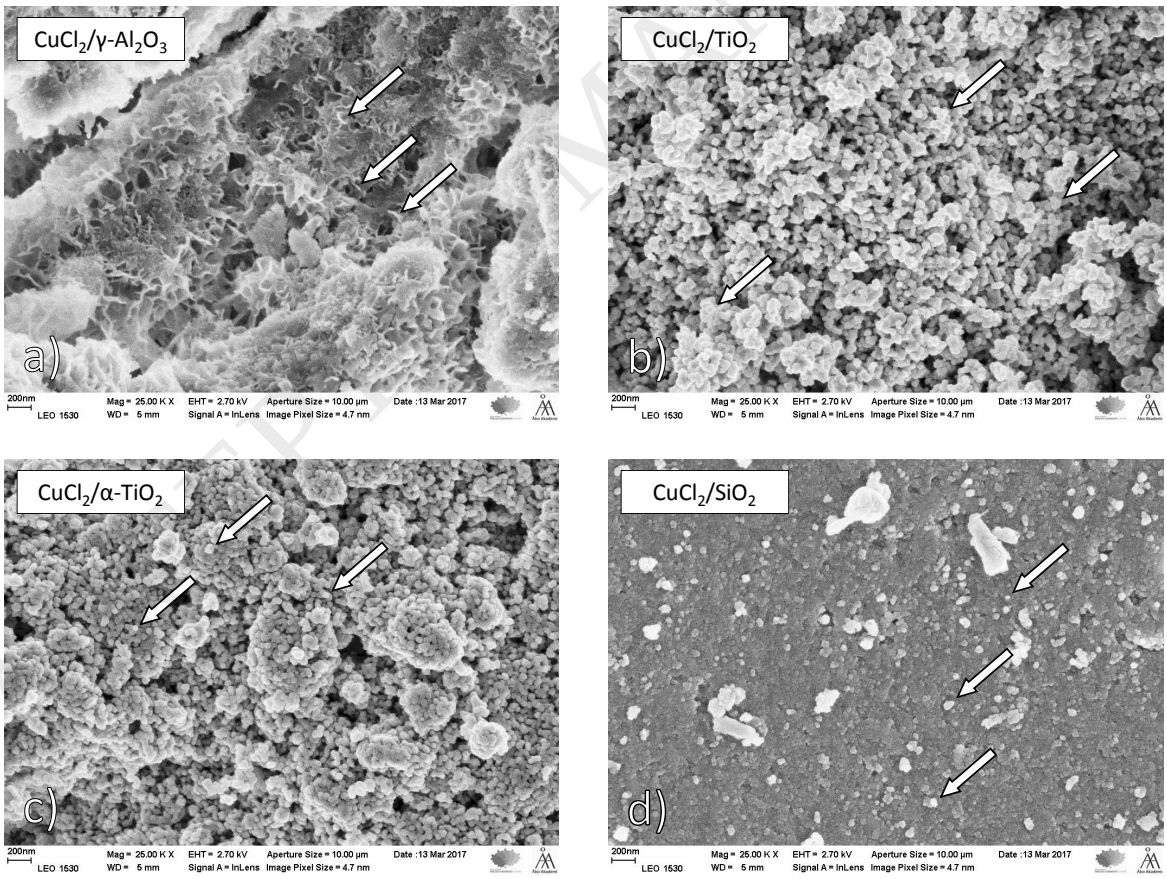

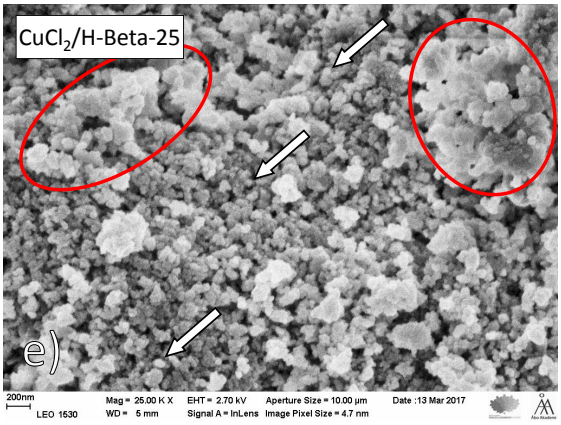

Figure 2. SEM: a) $CuCl_2/\gamma$-Al_2O_3, b) $CuCl_2/TiO_2$ (Hombikat), c) $CuCl_2/TiO_2$ (Alfa Aesar), d) $CuCl_2/SiO_2$, e) $CuCl_2$/H-Beta-25. Scale bar: 200 nm. The arrows point towards selected support crystallites and red circles show selected agglomeration of the phases for illustration purposes.

Figure 2 shows that the shape of Cu modified catalysts is cylindrical for $CuCl_2/\gamma$-Al_2O_3, spherical for $CuCl_2/TiO_2$ catalysts, while $CuCl_2/SiO_2$ exhibited an amorphous structure. Agglomeration of the phases into larger clusters was observed for $CuCl_2$/H-Beta-25 catalyst (red circles, Figure 2e).

Observation of $CuCl_2/SiO_2$ at higher magnification (scale bar: 20 µm, Figure 3) makes visible individual phases of the catalyst. It seems that light shapes correspond to Cu crystallites, while dark shapes related to pristine support crystallite. This assignment was confirmed by EDX analysis of the selected shapes for $CuCl_2/SiO_2$ catalyst.

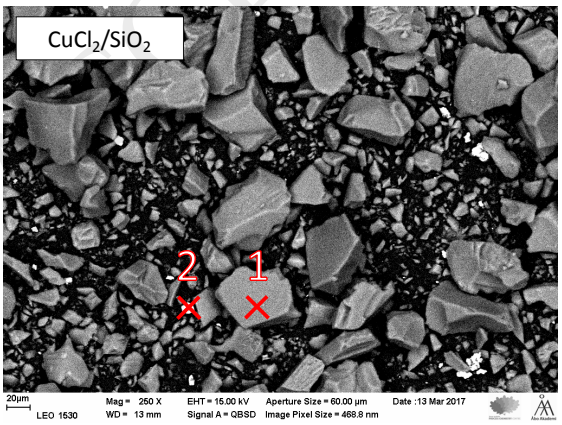

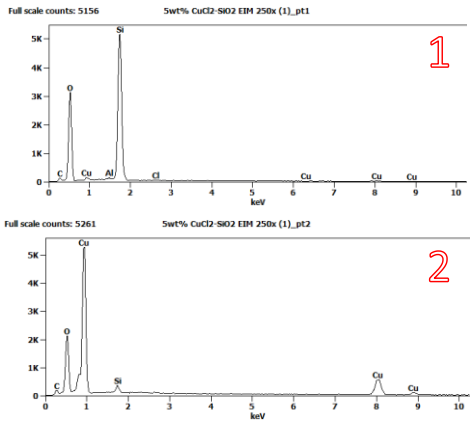

Figure 3. SEM-EDX:$CuCl_2/SiO_2$. Scale bar: 20 µm. The cross points towards selected support crystallites (point no. 1) and copper (point no. 2) for illustration purposes.

The particle sizes of copper in Cu-modified catalysts were studied using transmission electron microscopy (Figure 4). The Cu particle sizes calculated are given in Table 4. The smallest value for average of the copper particle size was obtained for the $CuCl_2/TiO_2$ (Hombikat) (2.6 nm). The $CuCl_2/TiO_2$ (Alfa Aesar) and $CuCl_2$/H-Beta-25 catalysts exhibited the second highest value (4.7 nm). The largest value for average of Cu particle size was obtained for $CuCl_2/\gamma$-Al_2O_3 catalyst (5.8 nm).

It is noteworthy to mention here, that the method of catalyst synthesis, evaporation impregnation was significant in the formation of small particle size of Cu (2.6 – 5.8 nm). However, besides method of catalyst synthesis, the structure of support was also important in resulting small Cu particles.

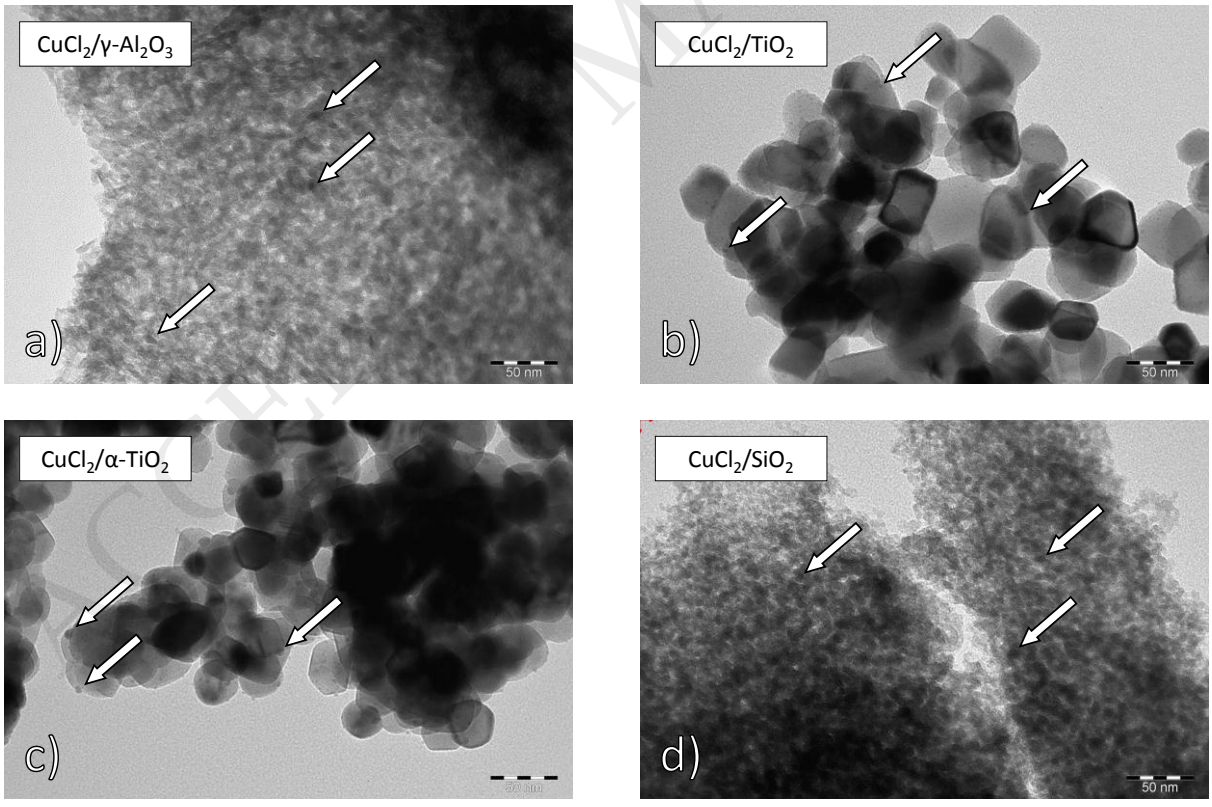

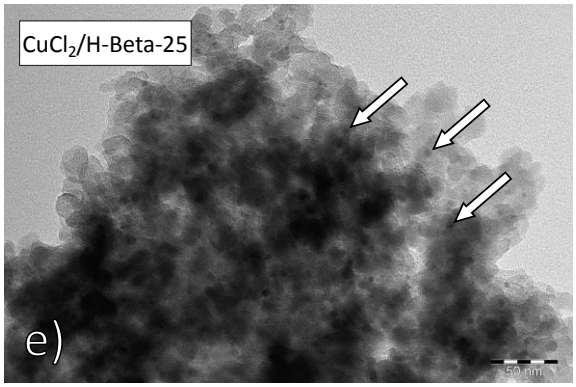

Figure 4. TEM: a) $CuCl_2$/ γ-Al_2O_3, b) $CuCl_2/TiO_2$ (Hombikat), c) $CuCl_2/TiO_2$ (Alfa Aesar), d) $CuCl_2/SiO_2$, e) $CuCl_2$/H-Beta-25. Scale bar: 50 nm. The arrows point towards selected copper particles for illustration purposes.

3.1.5 Effect of copper loading on support crystal structure

The phase proportions of the catalysts from XRD analysis is given in Table 5. The obtained phase weight proportions $W_i/\sum W$ for the measured samples was based on the Reitveld refinements. The quality of the Rietveld refinement fit is described by the parameter R_{exp}, where a smaller R_{exp} indicates a better fit to the measured data.

Peaks related to Al_2O_3 were observed in the diffractogram of $CuCl_2$/γ-Al_2O_3. Al_2O_3 was present as either γ- or η-Al_2O_3 phases or their combination. The $CuCl_2/TiO_2$ (Hombikat) contained TiO_2 anatase, TiO_2 rutile and CuO. The phase weight proportions were 74 ± 11%, 19 ± 11% and 7 ± 11%, respectively. The $CuCl_2/TiO_2$ (Alfa Aesar) contained TiO_2 anatase and CuO. The phase weight proportions were > 95% and < 5%, respectively. $CuCl_2/SiO_2$ contained CuO and possibly tetragonal SiO_2. The $CuCl_2$/H-Beta-25 contained beta zeolite polymorph A and CuO. The phase weight proportions were > 95% and < 5%, respectively.

Table 5. The crystal sizes and phase proportions of the catalysts from XRD analysis.

Catalyst	**Observed phase (framework)**	**$W_i/\sum W$**[1]	**R_{exp}**
	-	*%*	*%*
$CuCl_2$/γ-Al_2O_3	Al_2O_3 (γ or η)	n.a.	1.17
$CuCl_2/TiO_2$ (Hombikat)	TiO_2 anatase	74 ± 11	1.44

	TiO_2 rutile	19 ± 11	1.44
	CuO (monoclinic)	7 ± 11	1.44
$CuCl_2/TiO_2$ (Alfa Aesar)	TiO_2 anatase	> 95	1.42
	CuO (monoclinic)	< 5	1.42
$CuCl_2/SiO_2$	SiO_2 (tetragonal)[2]	n.a.	n.a.
	CuO (monoclinic)	n.a.	n.a.
$CuCl_2$/H-Beta-25	*BEA pol A (SiO_2)	> 95	1.09
	CuO (monoclinic)	< 5	1.09

[1] Phase detection threshold is approximately 5%

[2] Speculation based on a single, broad peak

The results of XRD analysis were not very useful for the identification of the structure, except $CuCl_2/TiO_2$ (Hombikat, Alfa Aesar) and $CuCl_2$/H-Beta-25 catalysts, where very weak peaks attributable to CuO have been found. Similar to the work of Leofanti et al. [10], this implies that the species present at high concentration and there must be in an amorphous state, or in the form of nanoclusters having a size below the detectable limit the diffraction technique. Although no $CuCl_2$ XRD peaks have been detected based on the literature data is reasonable to assume that $CuCl_2$ are the species prevailing at high copper concentration, together with minor amounts of paratacamite.

3.2 Evaluation of catalytic properties using copper-modified catalysts for ethylene oxychlorination

The efficiency of five different $CuCl_2$ catalysts with different physical-chemical properties was compared in ethylene oxychlorination. Figure 5 shows the ethene conversion while Figure 6 reveals selectivity to 1,2-dichloroethane (1,2-DCEA).

The highest conversion of ethylene (17.4 %) was achieved over $CuCl_2/\gamma$-Al_2O_3 at 250 °C, with the following products formed: 1,2-dichloroethane, ethyl chloride and vinyl chloride

(Table 6). The reason a higher conversion of ethylene over $CuCl_2/\gamma$-Al_2O_3 than with $CuCl_2/TiO_2$ (Hombikat, Alfa Aesar) catalysts can be attributed to a larger amount of acid sites in former catalyst compared to the latter one [20]. The highest conversion observed over $CuCl_2/\gamma$-Al_2O_3 can also be attributed to the presence of largest amount of basic sites (10.5 mmol/g) for this catalyst as compared to all the Cu-modified catalysts studied for oxychlorination reaction. The other plausible reason the highest conversion over $CuCl_2/\gamma$-Al_2O_3 catalyst is the particle size Cu (5.8 nm), the largest particle size as compared to $CuCl_2/TiO_2$, $CuCl_2/SiO_2$ and $CuCl_2$/H-Beta-25. On the contrary, $CuCl_2/SiO_2$ (0.3% at 250 °C) proved to be almost inactive, which might be related to less stabilization of the surface complexes than in $CuCl_2/\gamma$-Al_2O_3 catalyst [21].

The time on stream behaviour of ethene conversion and selectivity to 1,2-dichloroethane demonstrate a stable catalyst performance for $CuCl_2/\gamma$-Al_2O_3, $CuCl_2/TiO_2$ (Hombikat), $CuCl_2/TiO_2$ (Alfa Aesar) and $CuCl_2/SiO_2$. These measured data were steady and reproducible within the entire temperature range measured (200 – 250 °C). An exception is zeolite $CuCl_2$/H-Beta-25 for which continuous deactivation was observed over time, accompanied by an increasing selectivity to 1,2-DCEA.

The highest selectivity of 1,2-DCEA was achieved over $CuCl_2/TiO_2$ (Hombikat) (95.0% at 250 °C) and $CuCl_2/\gamma$-Al_2O_3 (95.5% at 200 °C). The largest increase in 1,2-dichloroethane selectivity was observed for $CuCl_2/TiO_2$ (Hombikat) is worth mentioning: for temperature increase form 200 °C to 225 °C, selectivity was increased from 31% to 82%.

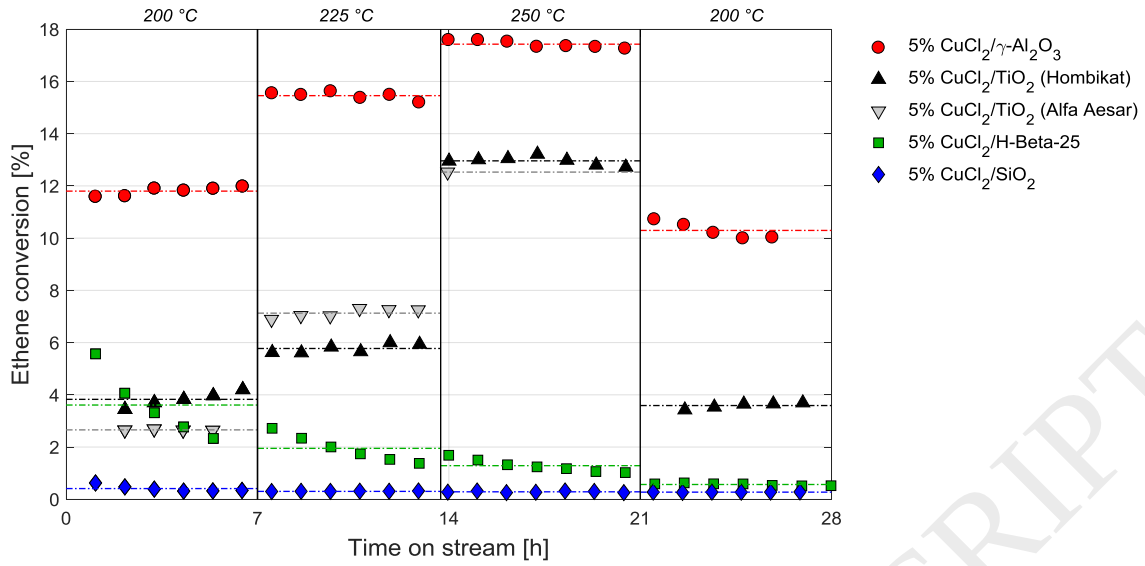

Figure 5. Oxychlorination of ethene: ethene conversion.

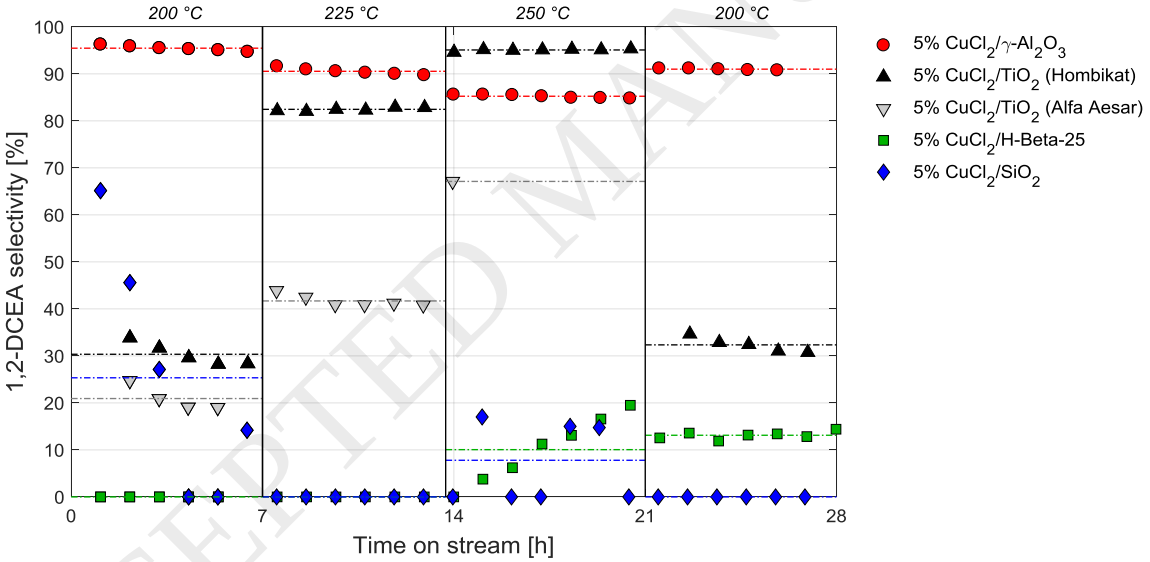

Figure 6. Oxychlorination of ethene: 1,2-DCEA selectivity.

The plausible explanation for the lowest ethylene conversion and the lowest selectivity for the desired product 1,2-dichlorethane over $CuCl_2/SiO_2$ and $CuCl_2$/H-Beta-25 catalysts can be attributed to catalyst acidity. This is consistent with the Figure 7 where the influence of catalyst acidity on turnover frequency is displayed. Figure 7 shows that the lowest values of frequency

turnover (more than $0.2 \cdot 10^{-5}$ s^{-1}) were achieved over $CuCl_2/SiO_2$ catalyst with extremely low amount of acid sites (less than 30 µmol/g) and also over $CuCl_2$/H-Beta-25 catalyst with very height amount of acid sites (more than 450 µmol/g). In contrast, high turnovers frequency (more than $1 \cdot 10^{-5}$ s^{-1}) values were achieved over catalysts with values of total catalyst activity between 50 and 350 µmol/g.

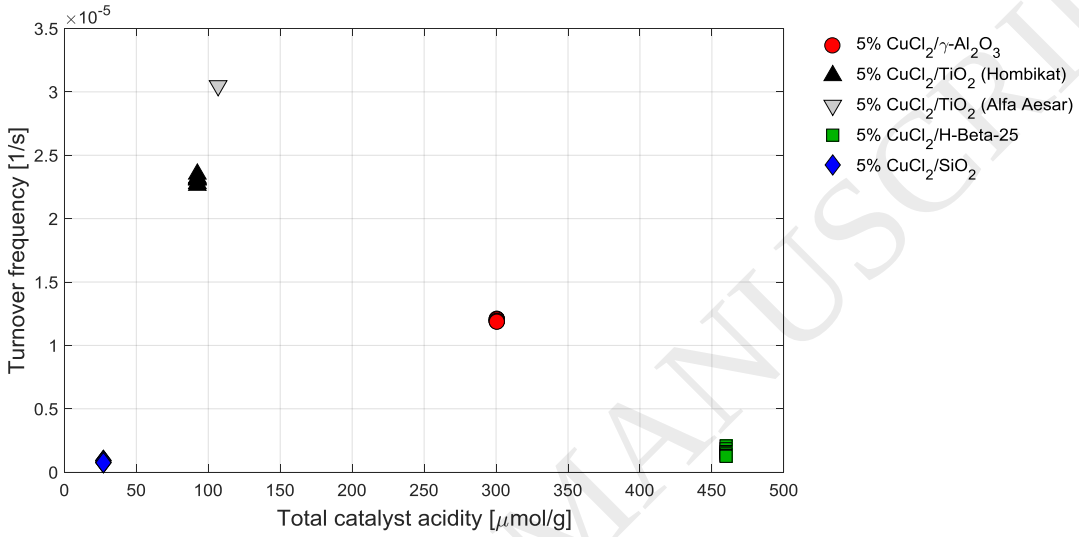

Figure 7. Oxychlorination of ethene: influence of acidity on turnover frequency.

A comparison of the experimental results of ethylene oxychlorination at 250 °C with the results from the literature are provided in Table 6. Different results of ethylene oxychlorination reflect different experimental conditions under which the reaction was performed (type of catalyst and its promoters, reaction temperature, composition of raw material, etc.). Compare to literature all catalysts in the current work were used without any promotors (e.g. K, Na, La).

Table 6. The comparison of results of the ethylene oxychlorination at 250 °C (Conversion, Yield, Selectivity in %).

Catalyst	**Cu**	**T**	**X, %**	**Yield, %**	**Selectivity, %**			**Ref.**
	wt.%	*°C*	*Ethene*	*1,2-DCEA EtCl*	*1,2-DCEA EtCl*	*VCl*	*Other by-*	

			conv.	$C_2H_4Cl_2$	C_2H_5Cl	$C_2H_4Cl_2$	C_2H_5Cl	C_2H_3Cl	*product*	
KCl-CeO_2-$CuCl_2$-cat.	n.a.	n.a.	98	n.a.	n.a.	n.a.	n.a.	55.4	n.a.	[3]
Commercial $CuCl_2$-cat.	n.a.	230	91	88	n.a.	97	n.a.	n.a.	3	[7]
$CuCl_2$/γ-Al_2O_3	5	250	41[1]	39	0.01	93	0.02	0.6	6	[2]
CeO_2-$CuCl_2$/Al_2O_3	*5*	230	30	n.a.	n.a.	n.a.	n.a.	n.a.	n.a.	[4]
Cu-K-La-Cl_x/ γ-Al_2O_3	7	200	10	10	0.0	100	0.0	0.0	0.0	[6]
$CuCl_2$/γ-Al_2O_3	5	230	10	10	n.a.	98	n.a.	n.a.	n.a.	[5]
$CuCl_2$/γ-Al_2O_3	5	250	**17.4**	14.9	2.5	85.2	14.4	**0.4**[2]	0.0	CW
$CuCl_2$/TiO_2 (Hombikat)	5	250	13.0	**12.4**	0.6	**95.0**	4.6	**0.4**[2]	0.0	CW
$CuCl_2$/TiO_2 (Alfa Aesar)	5	250	12.5	8.4	4.0	67.1	31.5	**0.5**[2]	0.0	CW
$CuCl_2$/H-Beta25	5	250	1.3	0.1	1.2	10.1	89.9	0.0	0.0	CW
$CuCl_2$/SiO_2	5	250	0.3	0.02	0.3	7.8	92.2	0.0	0.0	CW

[1]Ethylene conversion in pulse catalytic experiment

[2]VCl was observed only at reaction temperature 250 °C, at lower temperature was VCl selectivity equal zero

CW = current work

For the most promising materials Figure 8 shows influence of selectivity towards the desired product on ethene conversion. From the almost constant selectivity behaviour obtained on γ-Al_2O_3 as a catalyst support, a reaction network with two initial parallel reactions can be suggested, where one reaction is direct oxychlorination of ethylene to 1,2-DCEA, being the dominant one, while the second reaction is synthesis of ethyl chloride. At higher conversion of ethene and a higher reaction temperature, 1,2-DCEA is converted into vinyl chloride. In the graph, this is observed by a slight decrease 1,2-DCEA selectivity at higher conversion. On the contrary, from the results obtained on TiO_2 as a support, where selectivity increases with conversion, a network of consecutive reactions is much more prominent already at low conversion. First ethyl chloride is formed by ethene hydrochlorination followed by its subsequent transformation to 1,2-DCEA.

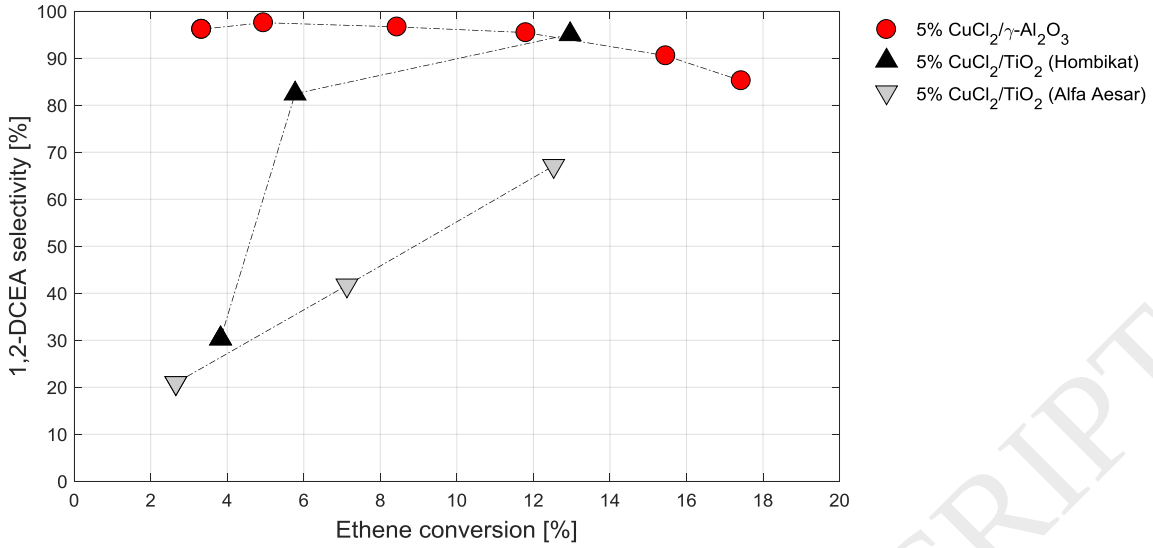

Figure 8 Oxychlorination of ethene: influence of 1,2-dichloroethane selectivity on ethene conversion.

In experiments with $CuCl_2/\gamma\text{-}Al_2O_3$, $CuCl_2/TiO_2$ (Hombikat) and $CuCl_2/TiO_2$ (Alfa Aesar) catalysts, 1,2-dichloroethane was detected as the main product. The other important product was EtCl. It seems that EtCl appears from the addition of HCl to ethylene, which can be catalyzed by the pristine support [2]. At higher temperatures, the formation of vinyl chloride by-product takes place. This fact is also described in the literature [2, 5]. The increase of selectivity to vinyl chloride at higher temperature could be related to successive conversion of 1,2-dichloroethane catalyzed by the Lewis and Brønsted acid sites on the support surface (with and without presence of the copper phase).

It is not possible to select one certain property of Cu modified catalysts (Table 7), which has the greatest impact on reaction products composition. The results of reaction one dependent on a combination of the properties of the support and its interactions with the catalyst active phase.

Table 7. The results of the characterization of Cu modified catalysts on different supports.

X		S		LAS		TAS		A_{cat}		V_{pore}		BAS		Cu		Cl/Cu		Cu	
% (at 250 °C)				µmol/g		µmol/g		m^2/g		cm^3/g		mmol/g		wt.%		at/at		g/100 m^2	
Al	**17**	**Ti-H**	**95**	B-25	285	B-25	460	B-25	827	Al	0.9	Al	10	Al	5.1	Al	0.44	Ti-A	0.103
Ti-H	**13**	**Al**	**85**	Al	229	Al	301	Si	275	B-25	0.7	Si	9	B-25	4.0	Si	0.15	Ti-H	0.096
Ti-A	13	Ti-A	67			Ti-A	107	Al	260	Si	0.5	B-25	6	Ti-H	3.0	Ti-H	0.10	Al	0.020
B-25	1.3	B-25	10			Ti-H	92	Ti-H	31	Ti-H	0.1	Ti-A	4	Ti-A	2.6	B-25	0.00	Si	0.009
Si	0.3	Si	8	Si	23	Si	27	Ti-A	26	Ti-A	0.1	Ti-H	4	Si	2.5	Ti-A	0.00	B-25	0.005

Al = $CuCl_2/\gamma$-Al_2O_3, Ti-H = $CuCl_2/TiO_2$ (Hombikat), Ti-A = $CuCl_2/TiO_2$ (Alfa Aesar), B-25 = $CuCl_2$/H-Beta-25, Si = $CuCl_2/SiO_2$

4 Conclusions

The results of the study clearly demonstrate that the nature of the catalyst support has a significant effect on both ethylene conversion and selectivity to 1,2-dichloroethane in oxychlorination over Cu modified catalysts. The difference in physical-chemical properties of supports was the reason for very different results (at 250 °C: 0.3 – 17.4% of ethylene conversion, 7.8 – 95% of 1,2-DCEA selectivity). All support materials were modified with 5 wt.% Cu, using the same evaporation impregnation procedure without any promotor.

As expected, very good results in terms of ethylene conversion and selectivity to 1,2-DCEA were achieved with a commonly used $CuCl_2/\gamma$-Al_2O_3 catalyst. The catalytic performance was stable in time on stream and had high reproducibility (with accuracy 1%). For the range of studied temperatures, the highest ethylene conversion was above 11.5% while selectivity to 1,2-DCEA exceeded 85%.

Very promising results have been achieved with Cu modified catalysts on TiO_2 supports (Hombikat and Alfa Aesar). The measured conversion over both types of catalysts were very similar in the whole measurement temperature range. On the contrary, significant differences were observed with respect to selectivity to 1,2-DCEA. This difference in selectivity increased with increasing reaction temperature (12% at 200 °C and 28% at 250 °C), and may be related to the composition of the support phases, anatase in TiO_2 (Alfa Aesar) and anatase + rutile in

TiO_2 (Hombikat). Cu modified catalysts on TiO_2 (Hombikat) support materials exhibited results comparable with alumina support with respect to ethene conversion at higher reaction temperatures. Even better results with $CuCl_2/TiO_2$ (Hombikat) catalyst (95% at 250 °C) than with $CuCl_2/\gamma$-Al_2O_3 (85% at 250 °C) were achieved in terms of selectivity to 1,2-DCEA. Compared with $CuCl_2/\gamma$-Al_2O_3, Cu modified catalysts on TiO_2 supports have much higher copper site density, but lower acidity, basicity, specific surface area, pore volume, Cl/Cu atomic ratio.

On the contrary, the results obtained with $CuCl_2/SiO_2$ or $CuCl_2$/H-Beta-25 catalysts were not very positive. The lowest ethene conversion (less than 0.4%) was achieved over $CuCl_2/SiO_2$ catalyst. Ethyl chloride was detected as the main product in the whole temperature range of the reaction. These results are consistent with extremely low Lewis acidity, copper site density and weak interactions between the active phase and the support.

$CuCl_2$/H-Beta-25 zeolite having very similar values of Lewis acid sites, total acidity, basicity, pore volume, copper site density, and Cl/Cu atomic ratio as $CuCl_2/\gamma$-Al_2O_3 catalyst gave a very low ethene conversion (less than 3.6%) and 1,2-DCEA selectivity (less than 10%). Moreover continuous deactivation was observed for this catalyst, accompanied by increasing selectivity to 1,2-DCEA. Low ethene conversion and observed behaviour over zeolite catalyst can be attributed to inhibiting active phase particle by agglomerating on the support that occurred during Cu impregnation.

5 Acknowledgments

The work is a part of the activities of Johan Gadolin Process Chemistry Centre (PCC), a centre of excellence financed by Åbo Akademi University. Financial support to Zuzana Vajglová from the Johan Gadolin Scholarship Programme is gratefully acknowledged.

6 References

1. Mile, B., T.A. Ryan, T.D. Tribbeck, M.A. Zammitt, and G.A. Hughes, *Kinetic Studies of the Dehydrochlorination of 1,2-dichloroethane on Alumina Supported Copper(II) Chloride Catalysts.* Topics in Catalysis, 1994. **1**(1-2): 153-162.
2. Finocchio, E., N. Rossi, G. Busca, M. Padovan, G. Leofanti, B. Cremaschi, A. Marsella, and D. Carmello, *Characterization and Catalytic Activity of $CuCl_2$-Al_2O_3 Ethylene Oxychlorination Catalysts.* Journal of Catalysis, 1998. **179**(2): 606-618.
3. Li, C., G.D. Zhou, L.P. Wang, S.L. Dong, J. Li, and T.X. Cheng, *Effect of Ceria on the MgO-gamma-Al_2O_3 supported CeO_2/$CuCl_2$/KCl catalysts for ethane oxychlorination.* Applied Catalysis A: General, 2011. **400**(1-2): 104-110.
4. Rout, K.R., E. Fenes, M.F. Baidoo, R. Abdollahi, T. Fuglerud, and D. Chen, *Highly Active and Stable CeO_2-Promoted $CuCl_2$/Al_2O_3 Oxychlorination Catalysts Developed by Rational Design Using a Rate Diagram of the Catalytic Cycle.* ACS Catalysis, 2016. **6**(10): 7030-7039.
5. Muddada, N.B., T. Fuglerud, C. Lamberti, and U. Olsbye, *Tuning the Activity and Selectivity of $CuCl_2$/gamma-Al_2O_3 Ethene Oxychlorination Catalyst by Selective Promotion.* Topics in Catalysis, 2014. **57**(6-9): 741-756.
6. Scharfe, M., P.A. Lira-Parada, V. Paunovic, M. Moser, A.P. Amrute, and J. Perez-Ramirez, *Oxychlorination-Dehydrochlorination Chemistry on Bifunctional Ceria Catalysts for Intensified Vinyl Chloride Production.* Angewandte Chemie-International Edition, 2016. **55**(9): 3068-3072.
7. Montebelli, A., E. Tronconi, C. Orsenigo, and N. Ballarini, *Kinetic and Modeling Study of the Ethylene Oxychlorination to 1,2-Dichloroethane in Fluidized-Bed Reactors.* Industrial & Engineering Chemistry Research, 2015. **54**(39): 9513-9524.
8. Flid, M.R., *Problems of Increase in the Selectivity of Ethylene Oxychlorination Processes: II. General Patterns in the Formation of Chloroorganic Byproducts in the Ethylene Oxychlorination Process.* Catalysis in Industry, 2016. **8**(1): 23-31.
9. Shi, D.Z., R.S. Hu, Q.H. Zhou, and C. Li, *Effect of Cr-Doping on $CuCl_2$-KCl-CeO_2/gamma-Al_2O_3 Catalysts for Ethane Oxychlorination.* Applied Catalysis A: General, 2015. **506**: 91-99.

10. Leofanti, G., M. Padovan, M. Garilli, D. Carmello, A. Zecchina, G. Spoto, S. Bordiga, G.T. Palomino, and C. Lamberti, *Alumina-Supported Copper Chloride 1. Characterization of Freshly Prepared Catalyst.* Journal of Catalysis, 2000. **189**(1): 91-104.
11. Gelperin, E.I., Y.M. Bakshi, A.G. Zyskin, Y.S. Snagovsky, and A.K. Avetisov, *Kinetics and Mechanism of Ethylene Oxychlorination.* Russian Chemical Industry, 1996. **28**(6): 12.
12. Baiker, A. and W.L. Holstein, *Impregnation Of Alumina With Copper Chloride-modeling Of Impregnation Kinetics And Internal Copper Profiles.* Journal of Catalysis, 1983. **84**(1): 178-188.
13. Flid, M.R., *Problems of Increase in the Selectivity of Ethylene Oxychlorination Processes: I. General Patterns in the Formation of Carbon Oxides in the Ethylene Oxychlorination Process.* Catalysis in Industry, 2015. **7**(2): 119-127.
14. Dollimore, D. and G.R. Heal, *An Improved Method for the Calculation of Pore Size Distribution from Adsorption Data*. Journal of Applied Chemistry, 1964. **11**: 109-114.
15. Horvath G. and K. Kawazoe. *Method for the Calculation of Effective Pore Size Distribution in Molecular Sieve Carbon*. Journal of Chemical Engineering of Japan, 1983. **16**: 470–475.
16. Emeis, C.A., *Determination of Integrated Molar Extinction Coefficients for Infrared-Adsorption Bands of Pyridine Adsorbed on Solid Acid Catalysts.* Journal of Catalysis, 1993. **141**(2): 347-354.
17. Weisz, P.B. and C.D. Prater, *Interpretation of Measurements in Experimental Catalysis.* Advances in Catalysis, 1954. **6**: 143-196.
18. Kubicka, D., N. Kumar, T. Venalainen, H. Karhu, I. Kubickova, H. Osterholm, and D.Y. Murzin, *Metal-Support Interactions in Zeolite-Supported Noble Metals: Influence of Metal Crystallites on the Support Acidity.* Journal of Physical Chemistry B, 2006. **110**(10): 4937-4946.
19. Leino, E., N. Kumar, P. Mäki-Arvela, A.-R. Rautio, J. Dahl, J. Roine, and J.-P. Mikkola, *Synthesis and Characterization of Ceria-Supported Catalysts for Carbon Dioxide Transformation to Diethyl Carbonate.* Catalysis Today, 2017, http://dx.doi.org/10.1016/j.cattod.2017.01.016
20. Goodwin, V., B. Yoosuk, T. Ratana, and S. Tungkamani, *Hydrotreating of Free Fatty Acid and Bio-Oil Model Compounds: Effect of Catalyst Support.* 2015 International Conference on Alternative Energy in Developing Countries and Emerging Economies, 2015. **79**: 486-491.

21.Zipelli, C., J.C.J. Bart, G. Petrini, S. Galvagno, and C. Cimino, *Study of $CuCl_2$ Supported on SiO_2 and Al_2O_3.* Zeitschrift Fur Anorganische und Allgemeine Chemie, 1983. **502**(7): 199-208.